

Microscopic phase separation in $\text{La}_2\text{CuO}_{4+x}$ induced by the superconducting transition

V. Yu. Pomjakushin

Joint Institute for Nuclear Research, 141980, Dubna, Moscow region, Russia

A. A. Zakharov

RSC "Kurchatov Institute," Kurchatov sq.1, 123182, Moscow, Russia

A. M. Balagurov

Joint Institute for Nuclear Research, 141980, Dubna, Moscow region, Russia

F. N. Gygax and A. Schenck

Institute for Particle Physics of ETH Zürich, CH-5232 Villigen PSI, Switzerland

A. Amato and D. Herlach

Paul Scherrer Institute (PSI), CH-5232 Villigen PSI, Switzerland

A. I. Beskrovny, V. N. Duginov, and Yu. V. Obukhov

Joint Institute for Nuclear Research, 141980, Dubna, Moscow region, Russia

A. N. Ponomarev

RSC "Kurchatov Institute," Kurchatov sq.1, 123182, Moscow, Russia

S. N. Barilo

Belorussian Institute of Semiconductors and Solid State Physics, 220072 Minsk, Belarus

(Received 16 April 1998)

The phase separation (PS) effect in superconducting $\text{La}_2\text{CuO}_{4+x}$ ($x \leq 0.04$) single crystals with low oxygen mobility was studied via μSR spectroscopy, high-resolution neutron diffraction, and magnetic susceptibility. Despite the fact that all crystals are inside the miscibility gap ($0.01 < x < 0.06$), only crystals with a sufficiently large excess oxygen concentration $x = 0.04$ show a macroscopic phase separation according to the neutron-diffraction data. However, in all samples a phase transition to an ordered magnetic state was observed by μSR spectroscopy concomitantly with the onset of superconductivity. This effect is treated as a microscopic phase separation which is possibly driven by superconductivity. [S0163-1829(98)02341-8]

Although the phenomenon of macroscopic phase separation (PS) in $\text{La}_2\text{CuO}_{4+x}$, was discovered in 1988,¹ it has not yet found a generally accepted explanation and the driving force of separation is still the subject of discussion. Recently, it was demonstrated that the repeatedly investigated (e.g., Ref. 2) phase diagram of $\text{La}_2\text{CuO}_{4+x}$, including the so called miscibility gap region $0.01 < x < 0.06$, is not universal. It has been unambiguously shown in the papers of A. Zakharov *et al.*³ and A. Balagurov *et al.*⁴ that along with the 'usual' $\text{La}_2\text{CuO}_{4+x}$ single crystals demonstrating the phase separation into oxygen-rich and oxygen-poor regions, it is possible to prepare crystals that are inside the miscibility gap and which show superconductivity without a macroscopic phase separation. The combined analysis of neutron and μSR data has shown that the phase-separation effect has an even more complicated behavior, namely, a macroscopically homogeneous superconducting crystal can be inhomogeneous on a microscopic level.⁵ Finally, we tentatively suggested in Ref. 6 that the appearance of a microscopic phase separation in $\text{La}_2\text{CuO}_{4+x}$ happens close to the superconducting transition temperature and, hence, can be connected with the formation of the superconducting and antiferromagnetic (AFM) states.

In this paper, we present additional experimental data on $\text{La}_2\text{CuO}_{4+x}$ single crystals, obtained by μSR and neutron diffraction, which allow us to clarify the problem. The most intriguing result is that we observed a coexistence of superconductivity and an ordered magnetic state without a macroscopic phase separation with essentially close transition temperatures. This is strong evidence in favor of the existence of the so called electronic phase separation in these crystals which is theoretically discussed in Refs. 7,8.

Two kinds of $\text{La}_2\text{CuO}_{4+x}$ superconducting crystals were studied: macroscopically homogeneous and phase-separated ones. The crystals were prepared by the molten solution method under thermodynamic equilibrium conditions. Details of crystal growth, oxygenating procedure, and high-resolution neutron-diffraction analysis are presented elsewhere.^{3,4} A specific feature of this series of crystals is the low oxygen mobility which for the crystals in the $x \leq 0.03$ region of miscibility gap results in the absence of a macroscopic phase separation by oxygen diffusion.

Below, we present data for two representative crystals: with $x = 0.02$ for the nonphase-separated series of samples (crystal A) with a superconducting transition temperature

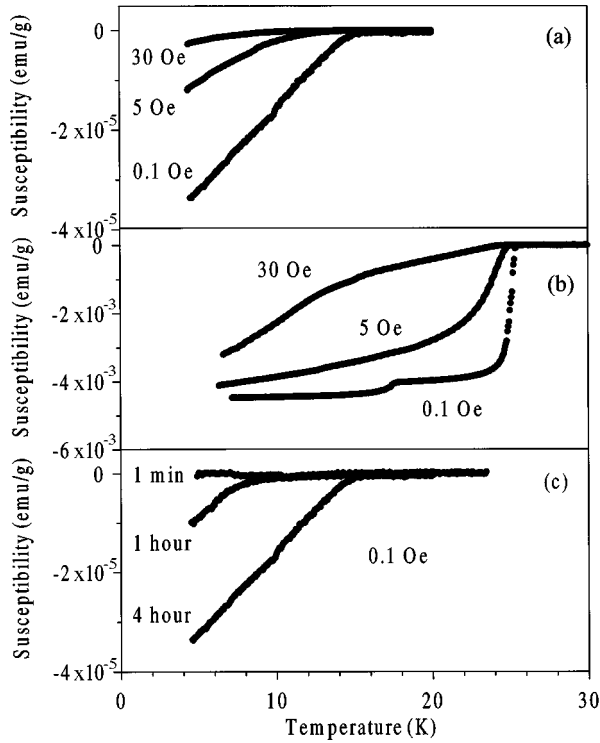


FIG. 1. The temperature dependence of the magnetic susceptibility for the $\text{La}_2\text{CuO}_{4.02}$ (a) and $\text{La}_2\text{CuO}_{4.04}$ (b) crystals in different magnetic fields, and (c) at different cooling rates from room temperature to 100 K for the $\text{La}_2\text{CuO}_{4.02}$ crystal. The magnetic field is parallel to the c axis of the crystal.

$T_c = 15$ K, and with $x = 0.04$ for the phase-separated samples (crystal B) with $T_c = 25$ K. The B crystal has been studied before by high-resolution neutron diffraction.⁴ The data on other crystals from these series differ only in minor details and support the main conclusions of the present work.

The μSR measurements were made using the General Purpose Spectrometer on the πM3 surface muon beam line at PSI (Villigen, Switzerland). The neutron-diffraction experiments were performed at the IBR-2 pulsed reactor of JINR (Dubna, Russia) with the high-resolution Fourier diffractometer⁹ and the DN-2 instrument equipped with a two-dimensional position-sensitive detector. The magnetization measurements were performed using a custom-made superconducting quantum interference device magnetometer.¹⁰

The magnetic susceptibility measured in external magnetic field of 0.1–30 Oe is presented in Fig. 1. The superconducting diamagnetic response in sample A with an onset transition temperature of $T_c = 15$ K is low and is suppressed by a small external field. However, superconducting state is not destroyed: the susceptibility remains negative and large in comparison with the paramagnetic contribution. The superconducting fraction is much larger in sample B and less sensitive to the applied magnetic field. We found that the diamagnetic response in sample A strongly depends on the cooling rate at the temperatures 100–300 K, where the oxygen diffusion can go [Fig. 1(c)]. Quenching (1 min from 300 down to 100 K) the sample to nitrogen temperatures suppresses the diamagnetism completely. This observation is evidence for the important role of oxygen diffusion and gives

an indirect confirmation that the system consists of small superconducting domains separated from each other by weak links which can be easily destroyed by a small magnetic field. The effect of quenching is considerably less pronounced in sample B. Similar effects for single crystals of $\text{La}_2\text{CuO}_{4+x}$ were observed earlier.^{2,11}

High-resolution neutron diffraction (with $\Delta d/d \approx 0.9 \times 10^{-3}$) revealed no trace of phase separation in sample A; neither splitting nor broadening of the neutron-diffraction peaks was observed, proving that, on a macroscopic scale, the homogeneous distribution of the excess oxygen in the crystal is preserved down to the lowest measured temperature (9 K). In sample B, the phase separation into oxygen-rich and oxygen-poor phases was observed clearly on cooling.⁴ The relative difference in the elementary lattice parameters of these two phases amounts to about 2×10^{-3} , which corresponds well with the results obtained for “usual” $\text{La}_2\text{CuO}_{4+x}$.¹ In crystal B, we observed the specific effect of diffraction peak broadening, the analysis of which allowed us to conclude that the average dimensions of the coherent regions of the coexisting phases are nearly the same and amount to 100 nm along the c axis and 150 nm within the plane. The phase separation process starts at $T = 250$ K and is complete at $T = 200$ K. It is worth mentioning that the two-step shape of the superconducting transition [Fig. 1(b)] is possibly connected with a network of coupled superconducting domains of macroscopic size, as mentioned above.

A magnetic state in crystal A was evidenced by the presence of a muon spin precession signal detected in zero external magnetic field (ZF- μSR) below 15 K. A correlated precession of the muon spins is possible only if the surrounding Cu moments are ordered coherently on the scale at least of a few lattice constants. The time dependence of the muon spin polarization $P(t)$, projected onto the axis of positron observation, can be described by the function

$$P(t) = a_1 \exp(-\lambda t) \cos(2\pi f_\mu t + \phi) + a_0 \exp(-\lambda_0 t), \quad (1)$$

where the precession frequency $f_\mu = \gamma_\mu B_\mu$ is given by the local magnetic field B_μ , acting on the muon which is proportional to the staggered magnetization of the copper magnetic moments; the precession amplitude a_1 is determined by the magnetically ordered volume fraction of the crystal and the direction of B_μ . The second component is the sum of the nonoscillating part of the muon polarization inside the magnetically ordered regions of the crystal and a contribution from the remaining paramagnetic volume. Typical ZF- μSR signals observed in sample A are shown in Fig. 2, where the difference between paramagnetic ($T = 30$ and 20 K) and the magnetically ordered ($T = 4$ K) states of the crystals can be clearly seen.

The amplitude a_1 assumed a constant value below 15 K, demonstrating that the magnetic transition is fully developed. The spontaneous muon-spin precession frequency f_μ is shown in Fig. 3(a) as a function of temperature. Its temperature dependence and low-temperature value $f_\mu = 5$ MHz are typical for the antiferromagnetic (AFM) state of stoichiometric $\text{La}_2\text{CuO}_{4+x}$,¹² suggesting that sample A displays the same AFM structure. Figure 3(b) shows the temperature de-

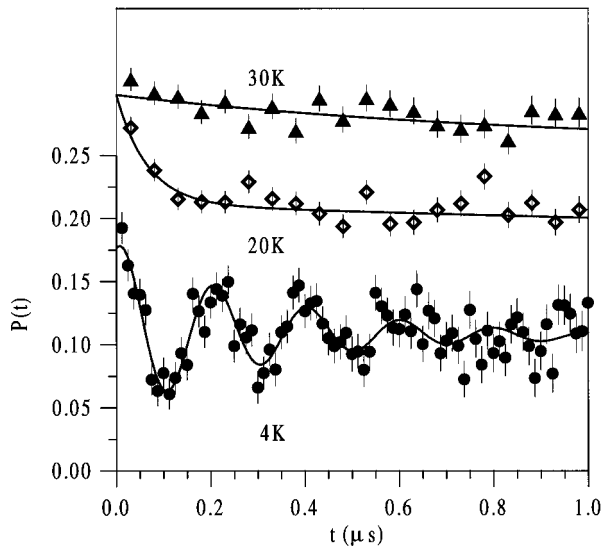


FIG. 2. Time dependence of the muon-spin polarization $P(t)$ in zero external field above and below the magnetic transition ($T_N = 15$ K) for $\text{La}_2\text{CuO}_{4.02}$. The data for $T = 20$ and 30 K are shifted up along the y axis.

pendence of the precession damping λ . It diverges as the temperature approaches 15 K. This means that the static AFM-correlated state is destroyed above $T_N = 15$ K. No precession signal was observed above 15 K; however, the polarization function possesses a fast decaying component which steadily decreases with increasing temperature up to

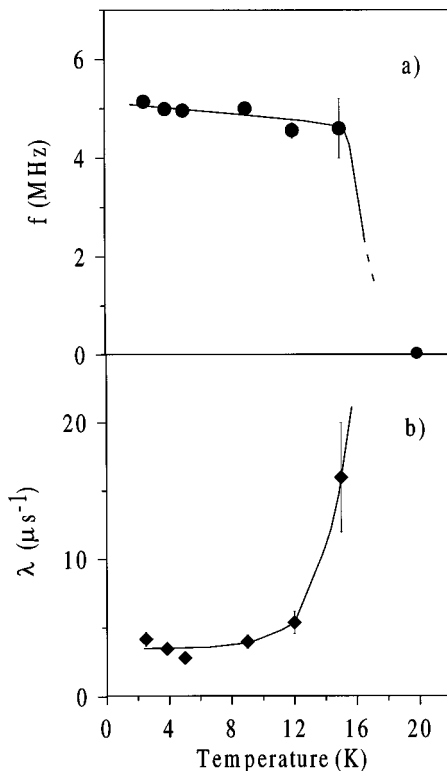


FIG. 3. The spontaneous muon-spin precession frequency f (a) and the precession damping λ (b) as a function of temperature in the $\text{La}_2\text{CuO}_{4.02}$ crystal.

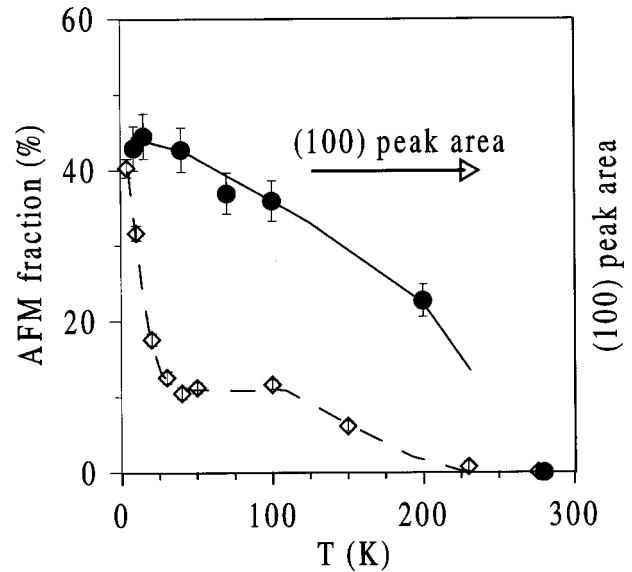


FIG. 4. The AFM volume fraction of the $\text{La}_2\text{CuO}_{4.02}$ crystal seen by μSR (the diamonds, left axis). The area of the (100) AFM peak as a function of temperature measured by neutron diffraction (circles, right axis) is also shown.

30 K (see Fig. 2). The origin of this fast depolarization is thought to reflect the slowing down of the Cu-spin fluctuations near the phase transition. Thus, the ZF- μSR data unambiguously prove the presence of static antiferromagnetic order in part of the crystal volume. The volume fraction occupied by the AFM phase amounts to $\geq 50\%$. This was determined from data measured in a transverse external field of 4 kOe in the temperature range of 3–280 K.

Unlike the sample A, sample B displays two characteristic temperatures associated with magnetic ordering. Below $T_{N1} \approx 230$ K, the AFM phase appears only in 10% of the crystal volume and under cooling to $T_{N1} \approx 25$ K, a sharp increase in the AFM fraction occurs, which reaches 40% at low temperatures (Fig. 4, left axis). The spontaneous muon-spin precession frequency detected below T_{N1} has, again, values of about 5 MHz for $T \rightarrow 0$ K, typical for AFM $\text{La}_2\text{CuO}_{4+x}$. The precession frequency smoothly increases with decreasing temperature, without any peculiarity at T_{N2} .

To check whether the observed transitions in samples A and B lead to a true long-range AFM order, we measured the neutron-diffraction spectra along the [100] direction ($Bmab$ space group) with the DN-2 instrument (Fig. 5). According to the μSR data, we expected to find the (100) magnetic peak below the magnetic transition below $T_N = 15$ K in sample A and below $T_{N1} = 230$ K in sample B. Indeed, in sample B, this peak was well visible, whereas in sample A, neutron diffraction revealed no traces of this reflection (inset in Fig. 5). The temperature dependence of the (100) peak area in sample B is shown in Fig. 4 (right axis). Since the copper magnetic moment does not change at T_{N2} , according to the temperature dependence of the muon-spin precession frequency, one would expect to find an increase in the (100) peak area below T_{N2} similar to the increase in the AFM fraction detected by μSR . However, neutrons do not see any peculiarity below $T_{N2} = 25$ K, whereas the muons see a

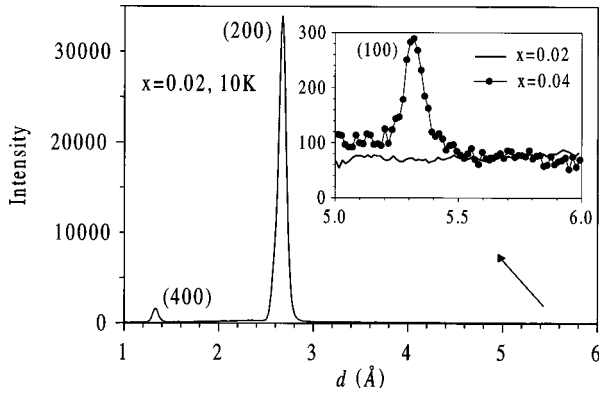


FIG. 5. The diffraction pattern from the [100] plane for $\text{La}_2\text{CuO}_{4.02}$ measured at $T=10$ K. The inset shows fragments of the diffraction patterns for both $\text{La}_2\text{CuO}_{4.02}$ and $\text{La}_2\text{CuO}_{4.04}$ near the (100) AFM peak. The position and intensity of the (200) and (400) peaks are close for both crystals.

fourfold increase in the AFM fraction. Hence, it seems that the magnetic Bragg peak is associated with those 10% of the sample volume which gives also rise to the spontaneous μSR signal below T_{N1} . As in sample A, we observe that the transition temperature T_{N2} , seen only by μSR , coincides with the superconducting transition temperature.

The main experimental results may be summarized as follows. In crystal A ($x=0.02$) the evolution of a correlated muon-spin precession starts at $T_N=15$ K, which coincides with the superconducting transition at T_c . Moreover, the crystal fraction occupied by the AFM phase is close to 50%. However, the magnetic state at low temperature does not possess true long-range order since the neutron-diffraction study failed to observe the relevant magnetic peak. In crystal B ($x=0.04$), the ordered magnetic state appears at $T_{N1} \approx 230$ K, which can be seen from both the μSR and neutron data. Down to the superconducting transition temperature, which coincides with $T_{N2}=25$ K, the volume fraction of the AFM phase is only $\sim 10\%$, which increases drastically up to $\sim 40\%$ upon further cooling. At the same time the fraction of the sample volume, occupied by the AFM phase with the correlation length sufficiently long to allow for the appearance of a magnetic Bragg peak, remains at the level of $\sim 10\%$ in the whole temperature range.

We will start our discussion of the experimental results with a brief sketch of the ‘‘temperature-concentration’’ phase diagram of $\text{La}_2\text{CuO}_{4+x}$. An earlier experimental study showed the presence of a miscibility gap in a rather wide concentration region. However, when a solid solution decomposes into two phases, two routes for the decay are possible: the nucleation and growth mechanism and/or the spinodal mechanism. Because there is an activation barrier in the former case, the process may be completely quenched in crystals with low mobility of the dopants. The spinodal decay does not need an activation process and, hence, inevitably leads to the development of spatial fluctuations in the composition through the sample. Our belief is that the different behavior of the crystals A and B arises from the different effective decomposition mechanisms: the $x=0.02$ crystal

does not have a high enough oxygen excess concentration to be in the spinodal region and has to split via the nucleation mechanism — which is not effective at low oxygen mobility. The oxygen excess concentration in the $x=0.04$ crystal, on the other hand, places the sample in the spinodal region and the decay develops independently of the oxygen mobility. We have carried out a comparative study of the ‘‘usual’’ $\text{La}_2\text{CuO}_{4+x}$ single crystal which has larger excess oxygen mobility. It is macroscopically separated into oxygen-rich and oxygen-poor phases which has large spatial dimensions (>2000 Å), and these phases possess ordinary antiferromagnetic and superconducting properties.¹³

We now discuss the two main experimental results of the present work: (i) the appearance (or sharp increase in the volume fraction) of the low-temperature AFM phase when the system enters the superconducting state and (ii) the invisibility of this AFM phase to neutron diffraction. We mention that a very similar phenomenon has been observed in a crystal with another oxygen concentration ($x=0.03$),⁵ where a magnetic transition to a short-range spin-glass-like state was observed to set in the vicinity of the superconducting transition.

One natural explanation for the observed behavior is that, after cooling, the crystals consist of domains of oxygen-rich and oxygen-poor phases of very small size (in the $x=0.04$ crystal, there are also metallic regions of larger size due to the macroscopic PS which produce a robust superconductivity at low temperatures). Then T_{N2} in crystal B corresponds to the Néel temperature of crystal A. The absence of AFM neutron reflections below these temperatures implies that the sizes of the coherent regions of this AFM phase are very small (of the order of several dozens Å) and, therefore, cannot be seen as Bragg reflections due to severe broadening.

The coincidence between the temperatures of the magnetic and superconducting transitions in quite different crystals, however, remains surprising. From the fact that the magnetic ordering temperatures $T_N=15$ K for $x=0.02$ (Fig. 2), $T_{N2}=25$ K for $x=0.04$ (Fig. 5), and $T_f=8$ K for $x=0.03$,⁵ are always close to the onset of the superconducting regime in all crystals, independent of their actual microstructure and characteristic temperatures, we may conclude that the magnetic ordering or the underlying microscopic PS is, in fact, induced by the superconducting transition. Such a behavior is predicted by a theoretical study⁷ in which it is found that a homogeneous metallic system becomes unstable in the presence of different competing electronic mechanisms, characterized by long-range or short-range correlations. There it was also shown that the stability regime is affected by the presence of superconducting pairing. As a result, the superconducting transition may cause a sample, homogeneously metallic in its normal phase, to split into weakly coupled metallic islands separated from each other by insulating interlayers which would possess the magnetic order.

The dependence of the diamagnetic response on the cooling rate even in macroscopically homogeneous crystals means that the redistribution of the extra oxygen atoms still exists, but on a microscopic scale. Since the oxygen microinhomogeneity can compensate the loss in Coulomb energy, the system becomes unstable towards an electronic phase separation. The phenomenon we found is, perhaps, not di-

rectly connected with the high-temperature superconductivity and can be a consequence of energy considerations, since both superconductivity and AFM lower the system energy on condition that Coulomb energy is compensated.

In summary μ SR and neutron-diffraction studies show that a microscopic phase separation (as opposed to macroscopic phase separation) in $\text{La}_2\text{CuO}_{4+x}$ single crystals with low oxygen mobility appears in parallel with superconduc-

tivity and is very likely driven by the formation of superconducting and AFM states.

The authors are grateful to V. G. Simkin and A. V. Polefor their help with neutron-diffraction measurements. The work was supported by the RFBR (Grant Nos. 960217431, 960217823), SNSF (Grant No. 7SUPJ048473), and by the HTSC national program (Grant No. 96019).

-
- ¹J. D. Jorgensen, B. Dabrowski, Shiyou Pei, D. G. Hinks, L. Soderholm, B. Morosin, J. E. Schirber, E. L. Venturini, and D. S. Ginley, *Phys. Rev. B* **38**, 11 337 (1988).
- ²F. C. Chou and D. C. Johnston, *Phys. Rev. B* **54**, 572 (1996).
- ³A. A. Zakharov, A. A. Nikonov, O. E. Parfenov, M. B. Tsetlin, V. M. Glaskov, N. V. Revina, S. N. Barilo, D. I. Zhigunov, and L. A. Kurnevitch, *Physica C* **223**, 157 (1994).
- ⁴A. M. Balagurov, V. Yu. Pomjakushin, V. G. Simkin, and A. A. Zakharov, *Physica C* **272**, 277 (1996).
- ⁵V. Yu. Pomjakushin, A. A. Zakharov, A. Amato, V. N. Duginov, F. N. Gygax, D. Herlach, A. N. Ponomarev, and A. Schenck, *Physica C* **272**, 250 (1996).
- ⁶V. Yu. Pomjakushin, A. Amato, A. M. Balagurov, A. I. Beskrovny, V. N. Duginov, F. N. Gygax, D. Herlach, A. N. Ponomarev, A. Schenck, V. G. Simkin, and A. A. Zakharov, *Physica C* **282-287**, 1353 (1997).
- ⁷V. J. Emery and S. A. Kivelson, *Physica C* **209**, 597 (1993).
- ⁸A. A. Gorbatshevich, Yu. V. Kopaev, and I. V. Tokatly, *JETP Lett.* **52**, 95 (1990); *Sov. Phys. JETP* **74**, 521 (1992); *Physica C* **223**, 95 (1994).
- ⁹V. L. Aksenov, A. M. Balagurov, V. G. Simkin, A. P. Bulkin, V. A. Kudryashev, V. A. Trounov, O. Antson, P. Hiismaki, and A. Titta, *J. Neutron Res.* **5**, 181 (1997).
- ¹⁰Yu. V. Obukhov, B. I. Saveliev, and V. V. Khanin, *Prib. Tekh. Eksp. (in Russian)* **5**, 166 (1991).
- ¹¹R. K. Kremer, A. Simon, V. Hizhnyakov, and E. Sigmund, *J. Magn. Magn. Mater.* **140-144**, 1285 (1995).
- ¹²Y. J. Uemura, W. J. Kossler, X. H. Yu, J. R. Kempton, H. E. Schone, D. Opie, C. E. Stronach, D. C. Johnston, M. S. Alvarez, and G. P. Goshorn, *Phys. Rev. Lett.* **59**, 1045 (1987).
- ¹³V. Yu. Pomjakushin *et al.* (unpublished).